Chemisorption-Driven Roughening of Hydrothermally Grown $KTa_{1-x}Nb_xO_3$ Nanoparticles

Supporting Information

Tiffany Ly[1], Jianguo Wen[2], and Laurence D. Marks[1]

[1]Department of Materials Science and Engineering, Northwestern University, Evanston, IL 60208

[2]Center for Nanoscale Materials, Argonne National Laboratory, Lemont, IL 60439

Niobium Oxide Formation Energies

The suitability of the parameters and functional used in the DFT calculations of surface energies were tested by calculating the formation energy of niobium (IV) oxide from niobium (V) oxide and niobium (II) oxide, i.e.:

$$Nb_2O_5 + NbO \rightarrow 3\ NbO_2$$

The same k-point mesh density, RMTs (RMT(O) = 1.25, RMT(Nb) = 1.71), and PBEsol functional were used. The space group and *k*-point mesh used for each material are provided in Table S1:

Table S1. Space group and *k*-point mesh used for the three niobium oxide phases to calculate the formation energy.

Material	**Space group**	***k*-point mesh**
Nb_2O_5	$I4_1/amd$	10×10×10
NbO	$Fm\bar{3}m$	13×13×13
NbO_2	$I4_1/az$	5×5×5

The formation energy of NbO_2 was calculated to be -61.4 kJ/mol. This agrees well with the enthalpy of formation calculated using experimental literature values, -65.7 kJ/mol.[1]

Reaction Kinetics

The different composition profiles between the KTN-1 and KTN-2 nanoparticles observed via EDS mapping may be explained by the different reaction kinetics of tantalum oxide and niobium oxide. The composition profiles can be related to the relative chemical potentials of the aqueous Ta and Nb species throughout each reaction, which are in turn related to the quantity of each species in solution. In the KTN-1 synthesis, the tantalum oxide formed a more reactive species in the KOH solution, thus the Ta species more readily reacted with KOH than Nb and became the first to be depleted, resulting in a final Nb-rich surface. In contrast, for the KTN-2 samples, the Nb species was initially deliberately made initially soluble by pre-dissolving Nb_2O_5 powder before the final reaction, which increased the Nb chemical potential in solution. The increased Nb chemical potential caused it to react first, leading to Ta enrichment of the final surface. It is probable that the Nb case involved the formation of an intermediate species stable in basic solutions, such as the Lindqvist ion ($Nb_6O_{19}^{8-}$).[2-4] When the Nb_2O_5 powder was pre-dissolved for the KTN-2 synthesis, it likely formed this species and reduced the number of reactions required for forming the final perovskite product. In contrast, when the same dissolving procedure was performed with Ta_2O_5 powder, the Ta_2O_5 remained solid, indicating that its aqueous form is less stable than that of Nb_2O_5, contributing to its higher reaction rate to forming the perovskite.

KTN-1 nanoparticles synthesized with different Ta_2O_5:Nb_2O_5 ratios confirmed that the states of the Ta and Nb species had more of an effect on the reaction kinetics than the amount of each. Figure S1 shows SE images and EDS maps of KTN-1 nanoparticles synthesized with a 1:3 (top) and 3:1 (bottom) ratio, which both exhibited the same composition gradient as KTN-1 nanoparticles synthesized with a 1:1 ratio. In all three cases, the bulk of the nanoparticles were Ta-rich, and the surfaces were Nb-rich.

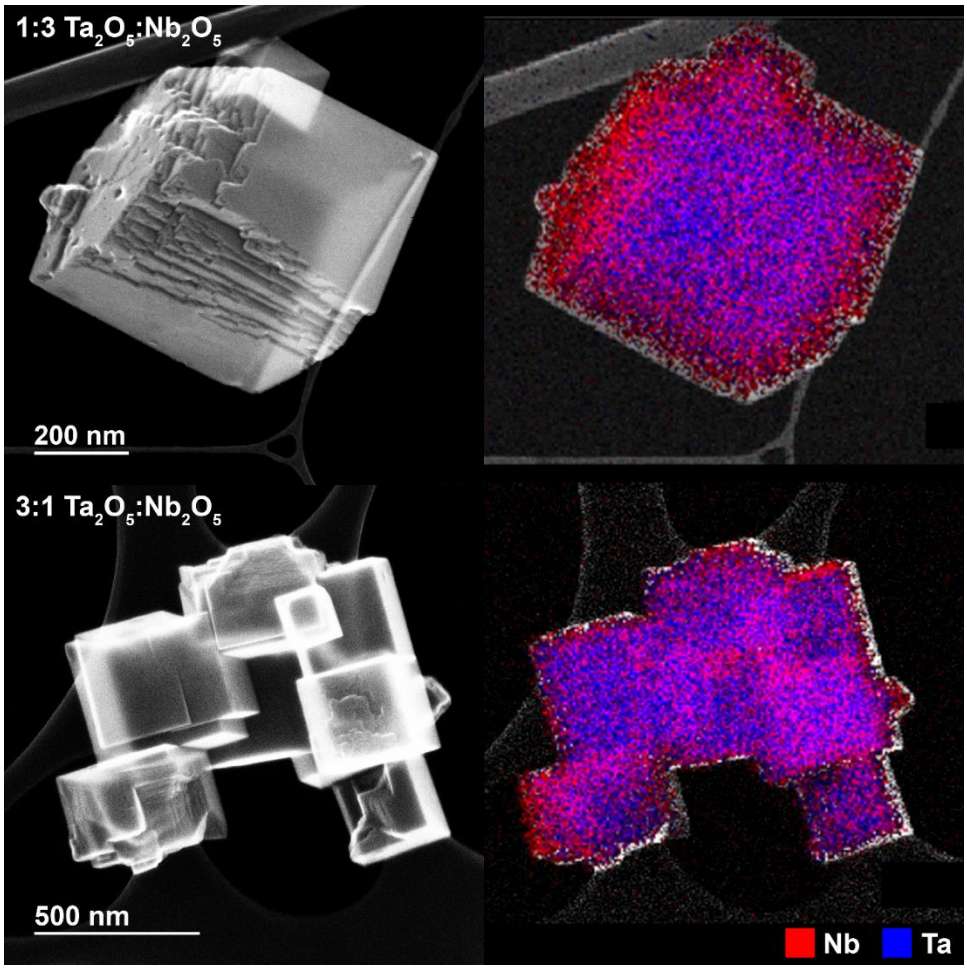

Figure S1. SE images and EDS maps of KTN nanoparticles synthesized following the KTN-1 procedure with different Ta_2O_5:Nb_2O_5 ratios (red is Nb, and blue is Ta). The top row shows a sample synthesized with a 1:3 ratio, and the bottom row shows a sample synthesized with a 3:1 ratio.

Surface Adsorption Characterization

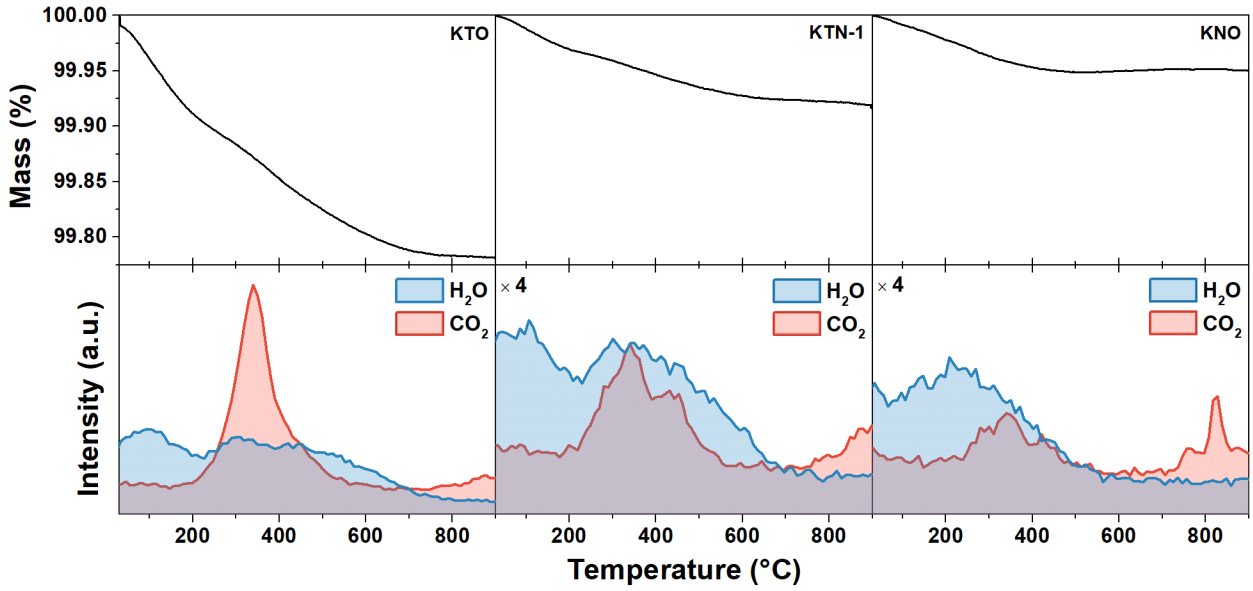

Figure S2. TGA-GC-MS analysis of KTO, KTN-1, and KNO nanoparticles.

Thermogravimetric analysis coupled with gas chromatography-mass spectrometry (TGA-GC-MS) was used to analyze the surface adsorption chemistry of the KTO, KTN-1, and KNO samples. TGA-GC-MS was performed on a Netzsch Jupiter F3 STA. The samples were heated from room temperature to 900 °C at a rate of 10 °C/min in nitrogen atmosphere. The results are plotted against temperature in Figure S2. The KTO sample experienced the most mass loss (0.22 %). In contrast, the KNO and KTN samples only underwent a 0.05 % and 0.08 % change, respectively. The GC-MS results show that in all three cases most of the mass loss may be attributed to adsorbed water and carbon dioxide species. Water loss occurred primarily between the temperatures of 30-600 °C, and carbon dioxide loss occurred between 200-550 °C. The water loss signal shows two distinct regions, one centered around 100 °C, and the other above 200 °C. These two regions may be attributed to physisorbed and chemisorbed water loss, respectively, because chemisorbed water has higher binding energies than physisorbed water. In the higher temperature region, the ratios of H_2O/CO_2 loss are 0.7, 1.2, and 1.1 for KTO, KTN, and KNO,

respectively. Because of the limitations established by the synthesis set-up and TGA-GC-MS instrument, it is difficult to prevent immediate adsorption of ex-situ species upon exposure to air and therefore also difficult to quantify the initial populations of adsorbed species on all the sample surfaces. However, the temperature dependent desorption of the overall species suggested that the Nb-rich surfaces of KTN-1 and KNO have significant water chemisorption.

References

1. Chase, M. W., Jr. Nist-Janaf Thermochemical Tables, Fourth Edition. *J. Phys. Chem. Ref. Data, Monograph 9* **1998**, 1-1951.
2. Jehng, J.-M.; Wachs, I. E. The Molecular Structures and Reactivity of Supported Niobidum Oxide Catalysts *Catal. Today* **1990**, *8*, 37-55.
3. Nyman, M.; Alam, T. M.; Bonhomme, F.; Rodriguez, M. A.; Frazer, C. S.; Welk, M. E. Solid-State Structures and Solution Behavior of Alkali Salts of the $[Nb_6O_{19}^{8-}$ Lindqvist Ion. *J. Cluster Sci.* **2006**, *17*, 197-219.
4. Goh, G. K. L.; Lange, F. F.; Haile, S. M.; Levi, C. G. Hydrothermal Synthesis of $KNbO_3$ and $NaNbO_3$ Powders. *J. Mater. Res.* **2003**, *18*, 338-345.